Electronic Supplementary Material (ESI) for Catalysis Science & Technology.


# SUPPORTING INFORMATION

## Evaluating metal oxide support effects on the RWGS activity of $Mo_2C$ catalysts

Cameron F. Holder[a*], James R. Morse[a], Patrick M. Barboun[b], Andrew R. Shabaev[a], Jeffrey W. Baldwin[c], Heather D. Willauer[a]

[a] Materials Science and Technology Division, Naval Research Laboratory, Washington, D.C. 20375, USA

[b] NRC Postdoctoral Research Associate, Naval Research Laboratory, Washington, D.C. 20375, USA

[c] Acoustics Division, Naval Research Laboratory, Washington, D.C. 20375, USA

* Corresponding Author at: Naval Research Laboratory, Washington, D.C. 20375, USA

*Email address:* cameron.holder@nrl.navy.mil

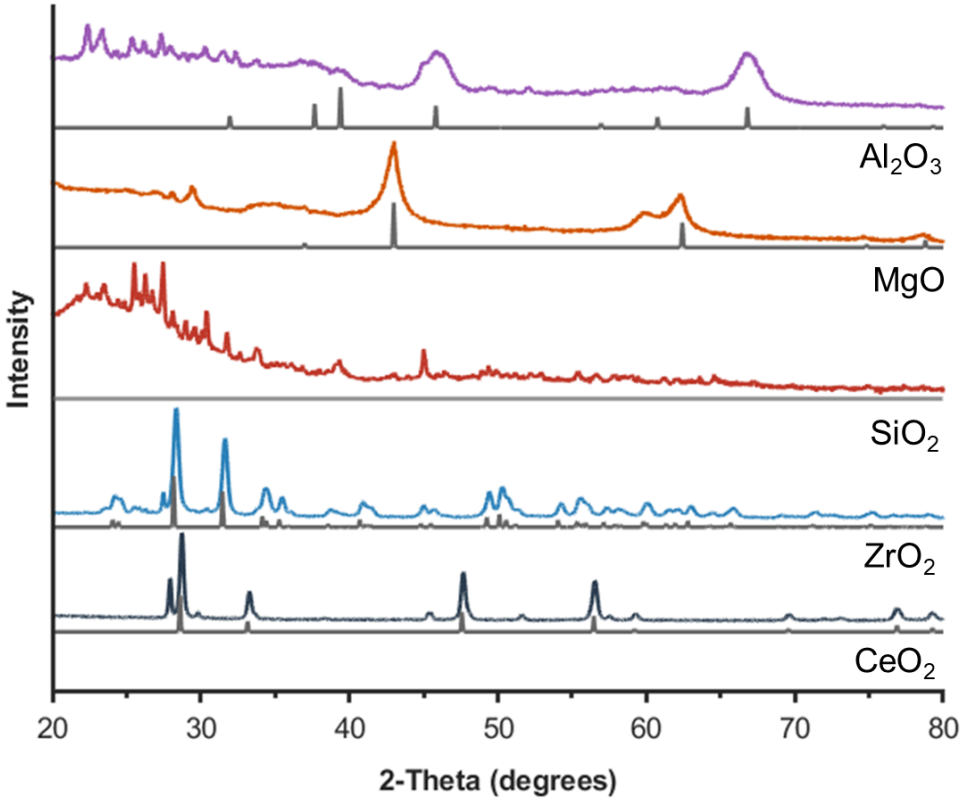


**Fig. S1** XRD patterns post-calcination depicting formed molybdenum oxides on the various metal oxide supports. The experimental patterns are shown in color while the corresponding metal oxide reference patterns are shown in gray.

**Table S1** Molybdenum oxides identified by XRD post-calcination for each support.

| Material | Molybdenum Oxides |
|---|---|
| $Al_2O_3$ | $K_2MoO_4$, $KAl(MoO_4)_2$, $MoO_3$ |
| $SiO_2$ | $K_2Mo_4O_{13}$, $MoO_3$ |
| MgO | $K_{10}Mg(Mo_7O_{27})$ |
| $ZrO_2$ | $Zr(MoO_4)_2$, $K_2MoO_4$, $MoO_3$ |
| $CeO_2$ | $KCe(MoO_4)_2$ |

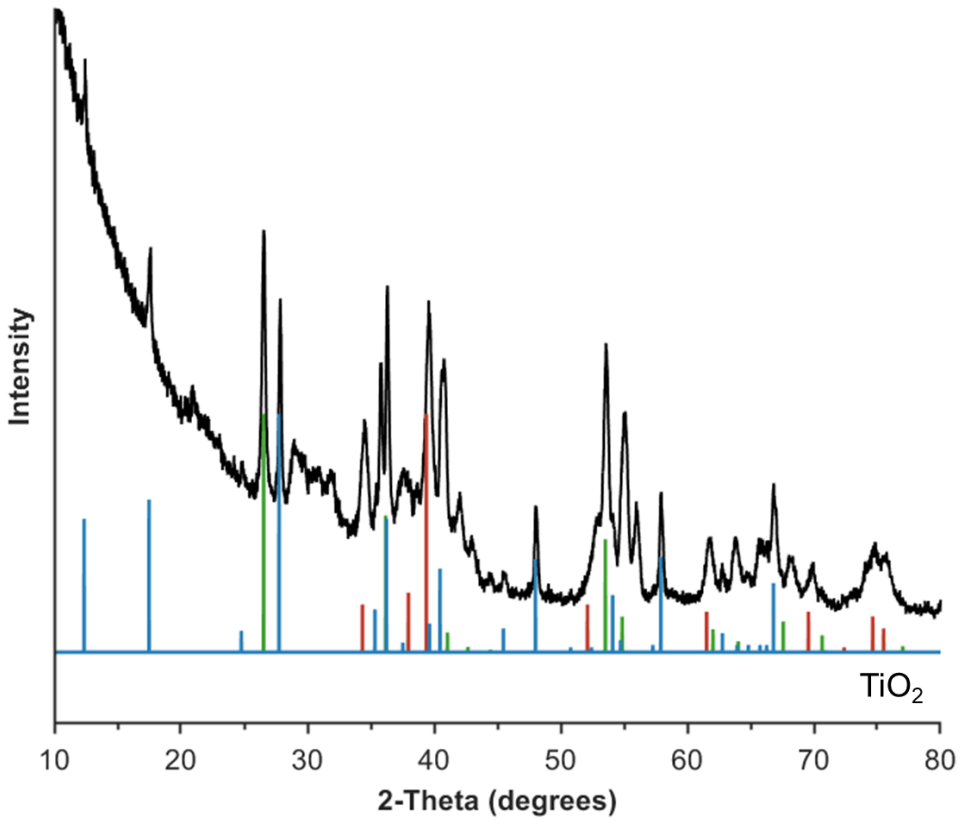


**Fig. S2** Experimental XRD pattern of K-$Mo_2C/TiO_2$ (black) with the associated reference patterns of $TiMoO_4$ (green), $KTi_4O_8$ (blue), and $Mo_2C$ (red). The remaining unidentified peaks could not be matched to a reference pattern but are most likely ascribed to other molybdenum or titanium-base metal oxides.

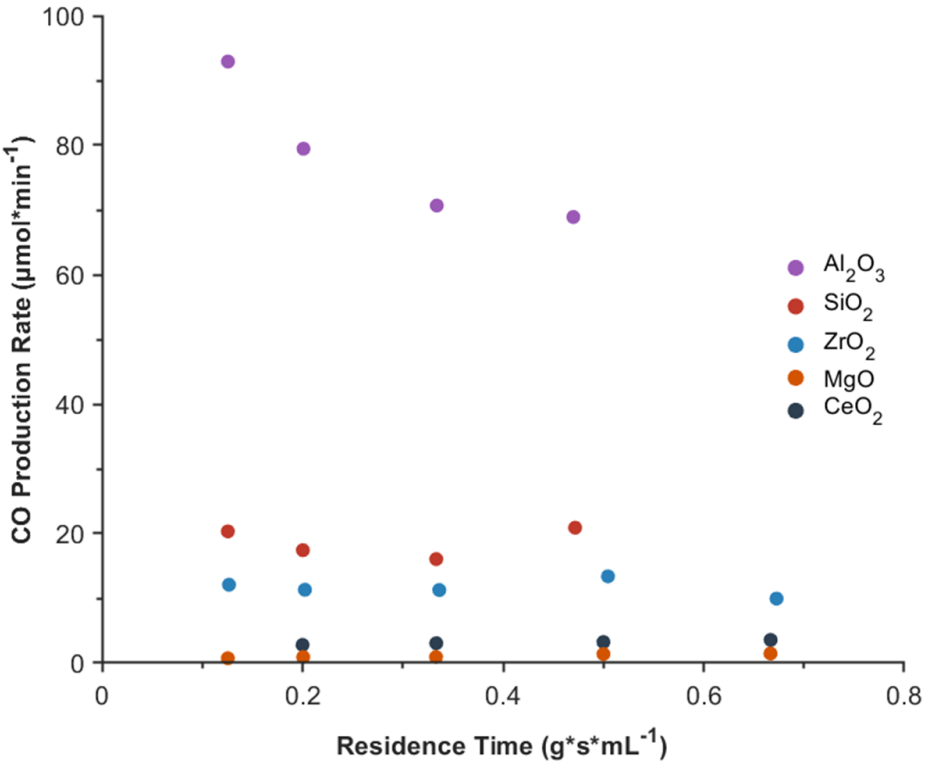


**Fig. S3** The production rate of CO as a function of residence time for K-$Mo_2C$ supported on various metal oxide supports. The CO turnover frequency was extracted from the y-intercept of the best fit line that was generated from data points at the three lowest residence times for each catalyst/support system.

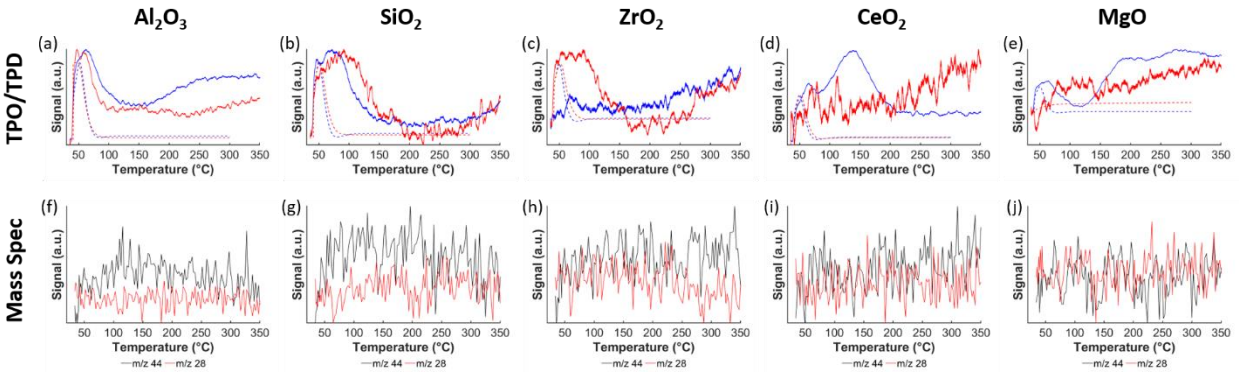


**Fig. S4** Temperature programmed oxidation (solid lines) and temperature programmed desorption (dashed lines) experiments for the bare metal oxide supports (blue) and supported K-$Mo_2C$ materials (red) are shown in the top row. The corresponding mass spectra for m/z 44 and 28 are shown in the bottom row for supported K-$Mo_2C$. No significant increase in m/z 28 signal was observed indicating that either $Mo_2O_xC_y$ was not formed or the subsequent formation of CO was below the detectable limits of the mass spectrometer.

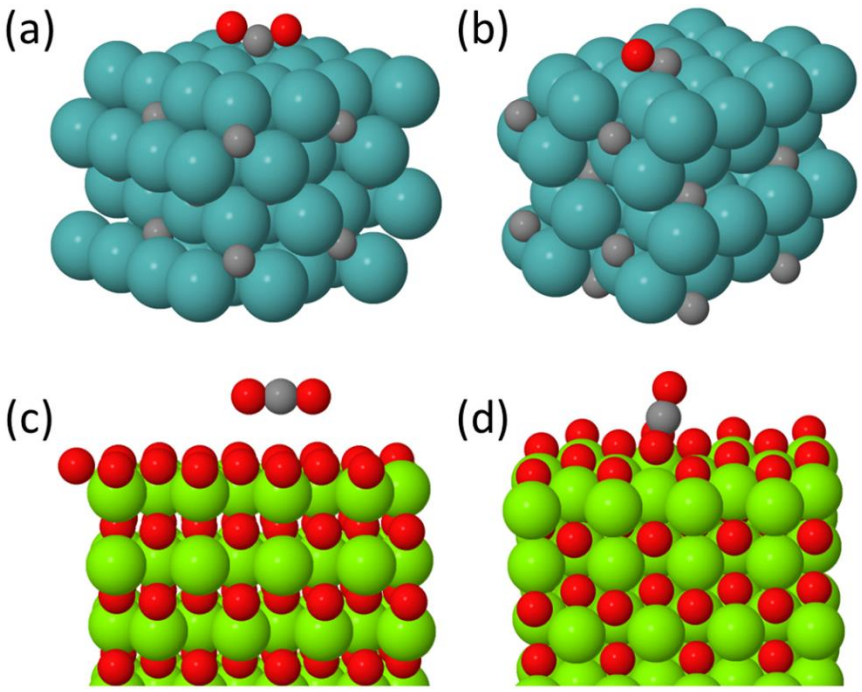


**Fig. S5** Computational models showing the interaction of $CO_2$ and CO when placed on bulk slabs of (a,b) $Mo_2C$(100) and (c,d) MgO(111). The green spheres represent Mg, the red spheres represent O, the blue spheres represent Mo, and the gray spheres represent carbon.

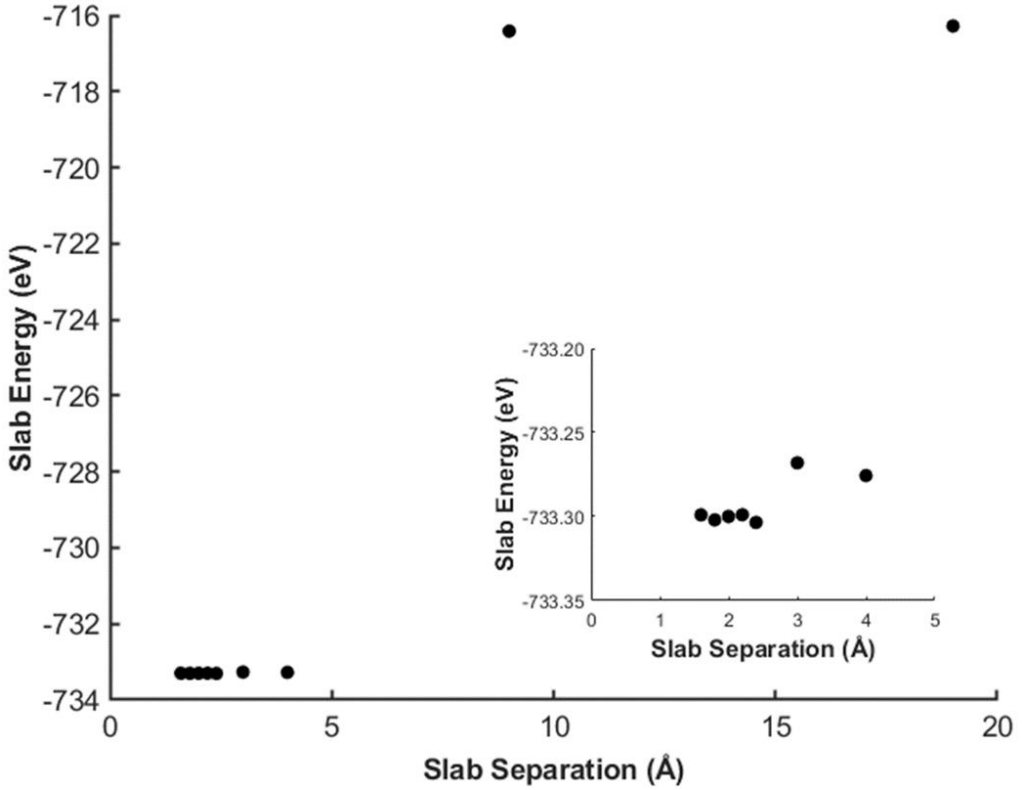


**Fig. S6** Relaxed energies of the combined slabs at various initial separation distances for $Mo_2C$(100) and the O-terminated MgO(111) slabs. The inset shows a magnified region at lower initial slab separation distances. For initial separation distances less than 4 Å, the relaxed structure showed a separation distance of approximately 1.5 Å.

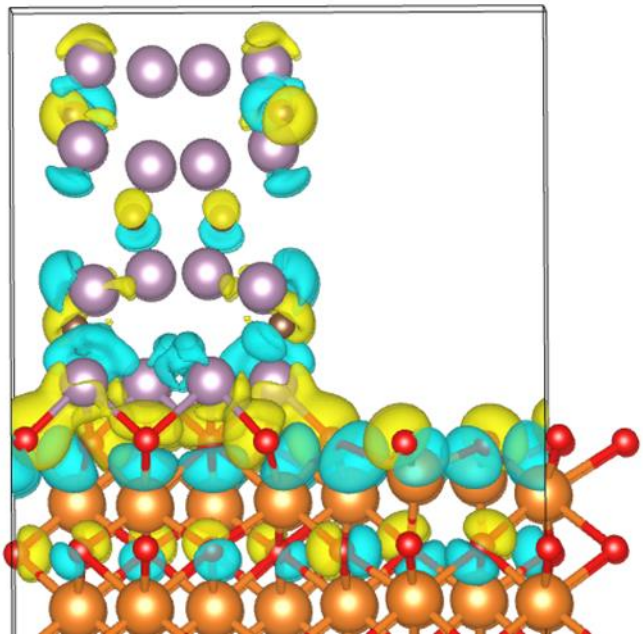

**Fig. S7** Charge density difference of the $Mo_2C$(100) ribbon on top of the O-terminated MgO(111) slab. The yellow isosurfaces are indicative of areas with increased electron density whereas the blue isosurfaces indicate areas with decreased electron density.